Search for a dark photon and an invisible dark Higgs boson in $\mu^+\mu^-$ and missing energy final states with the Belle II experiment

Belle II Collaboration

This material is submitted as supplementary information for the Electronic Physics Auxiliary Publication Service. We provide an additional text file with numerical results of the expected background events, signal efficiency, observed yields, observed 90% CL upper limit on the cross section of $e^+e^- \to A'\,h'$ with $A' \to \mu^+\mu^-$ and h' invisible as well as of the observed 90% CL upper limit on $\varepsilon^2 \times \alpha_D$ as functions of $M_{A'}$ and $M_{h'}$.

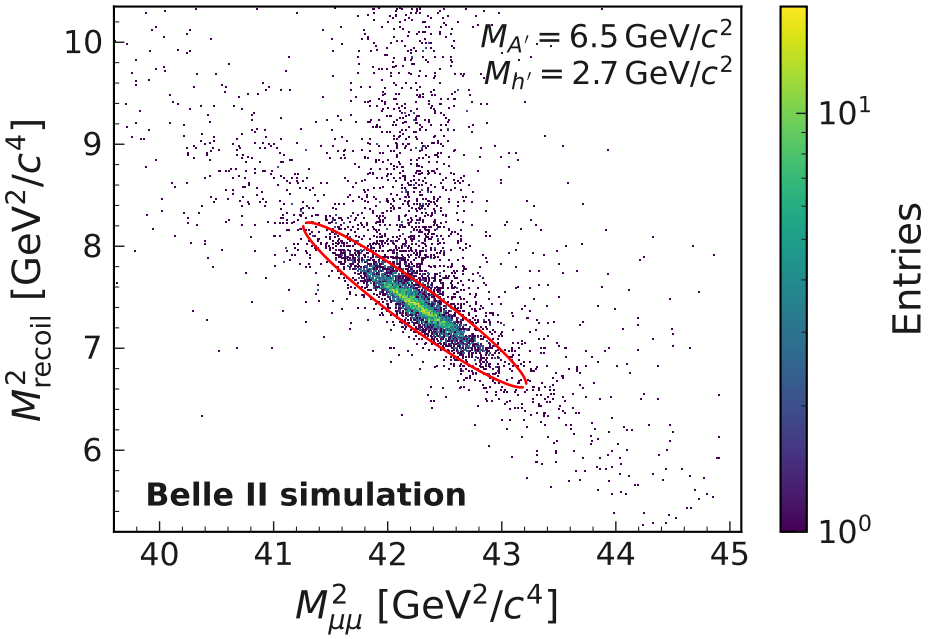

FIG. S1: Example of a two-dimensional squared mass distribution for a given signal hypothesis ($M_{A'}$=6.5 GeV/c^2, $M_{h'}$=2.7 GeV/c^2). The upward tail in the squared recoil mass distribution is due to ISR. Also shown is the elliptical search window contour.

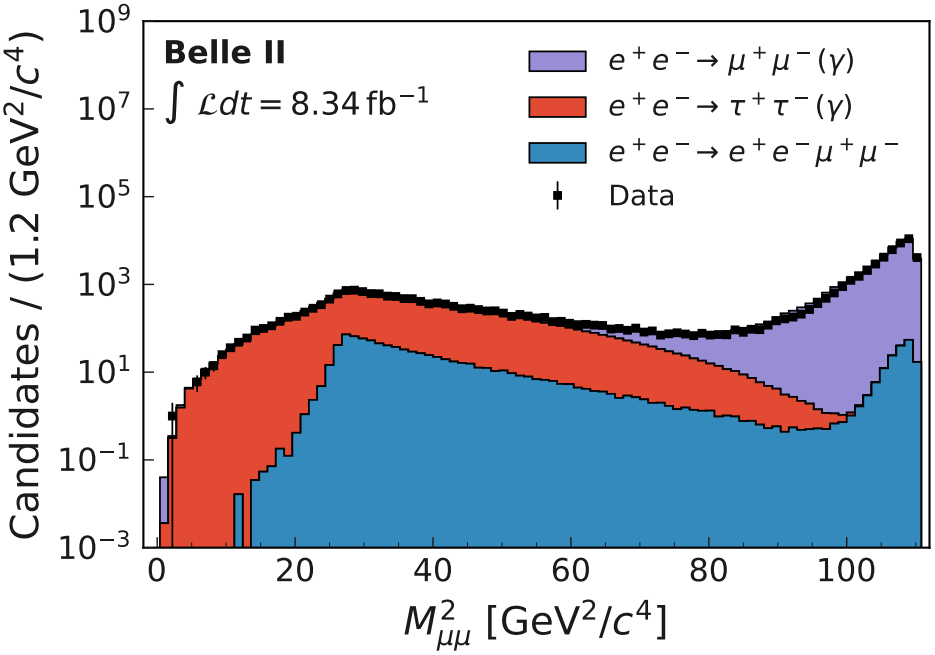

FIG. S2: Squared dimuon mass $M^2_{\mu\mu}$ distribution in data and simulation, before the C_η selection. Background contributions are stacked.

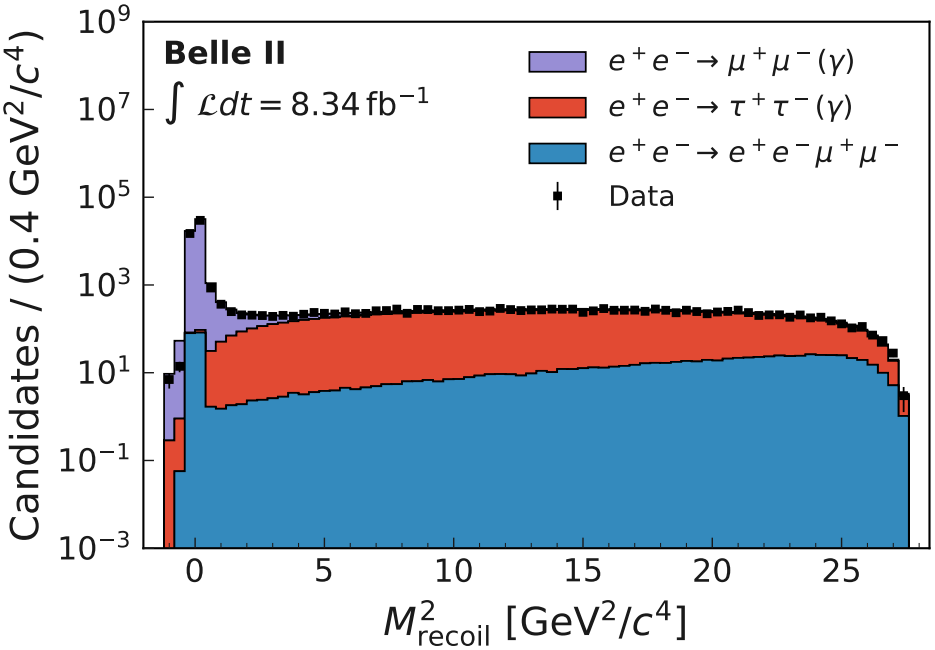

FIG. S3: Squared recoil mass M^2_{recoil} distribution in data and simulation, before the C_η selection. Background contributions are stacked.

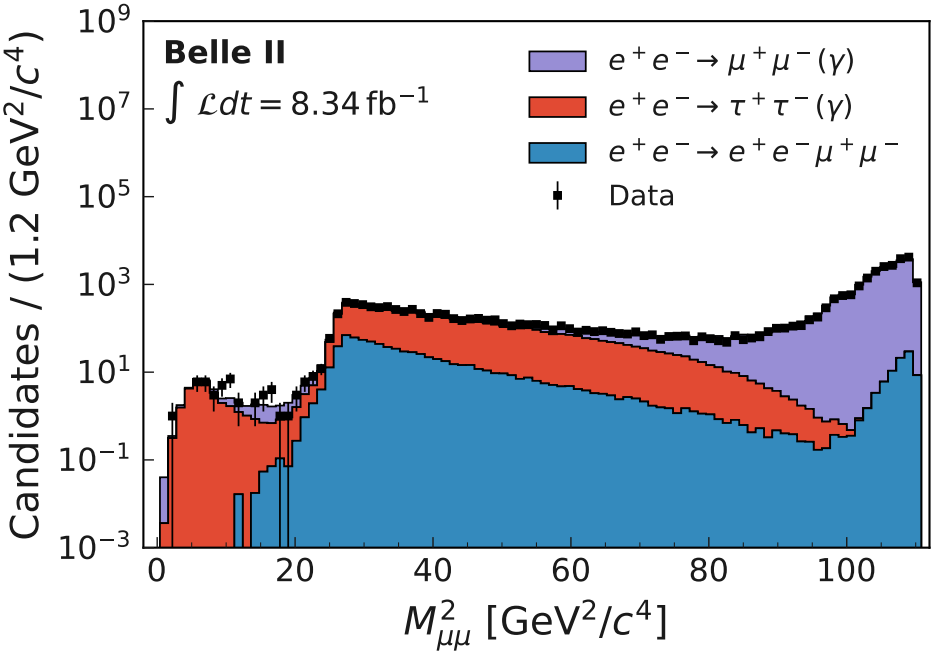

FIG. S4: Squared dimuon mass $M^2_{\mu\mu}$ distribution in data and simulation, after the C_η selection. We show here events that pass the selection in at least one of the search windows in which they are contained: this choice is motivated by the fact that the C_η selection is defined at search window level and windows overlap. Background contributions are stacked.

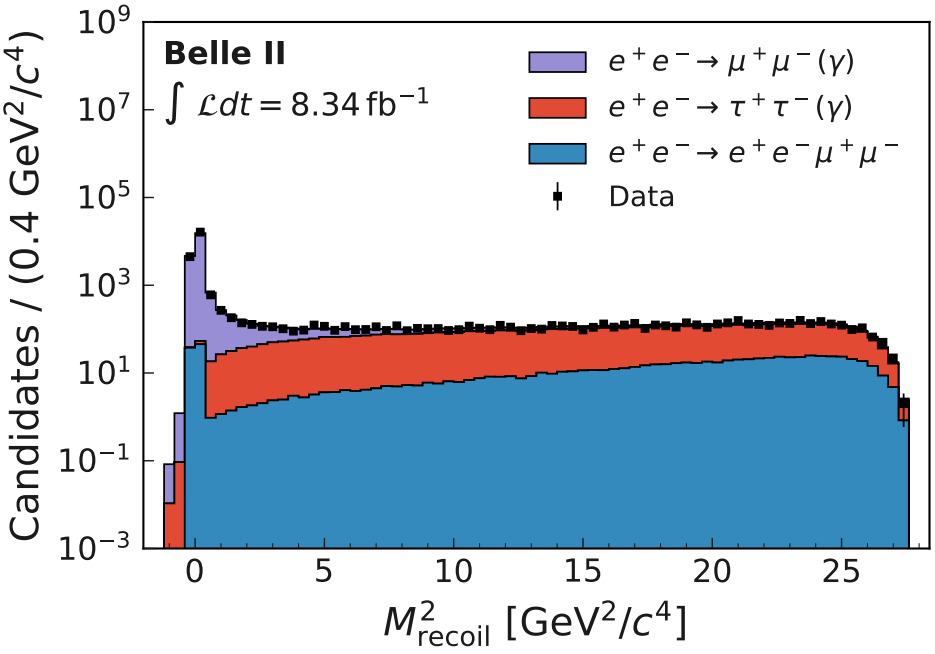

FIG. S5: Squared recoil mass M^2_{recoil} distribution in data and simulation, after the C_η selection. We show here events that pass the selection in at least one of the search windows in which they are contained: this choice is motivated by the fact that the C_η selection is defined at search window level and windows overlap. Background contributions are stacked.

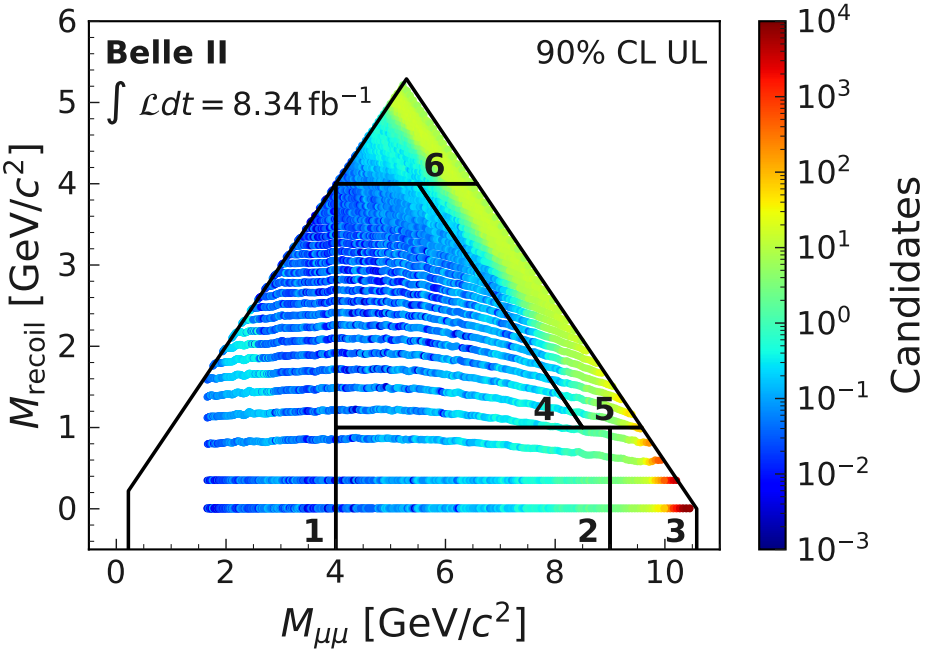

FIG. S6: Expected event counts inside the search windows after all selection criteria. Points correspond to search window centers. Macroregion boundaries are also shown.

TABLE I: Expected and observed events in macroregions after all selection criteria. We count here events that pass the selections in at least one of the search windows in which they are contained: this choice is motivated by the fact that the C_η selection is defined at search window level and windows overlap. The dominant [subdominant, when not negligible] background source in each macroregion is also indicated. Uncertainties on expected events are from luminosity and simulation sample size.

Macroregion	Expected events	Observed events	Dominant background
1	37.0 ± 0.7	35	$\tau^+\tau^-(\gamma)$
2	75.5 ± 1.7	72	$\mu^+\mu^-(\gamma)$
3	20779 ± 210	21399	$\mu^+\mu^-(\gamma)$
4	65.1 ± 1.4	71	$\mu^+\mu^-(\gamma)$ [$\tau^+\tau^-(\gamma)$]
5	4150 ± 42	4085	$\tau^+\tau^-(\gamma)$ [$\mu^+\mu^-(\gamma)$]
6	3379 ± 34	3323	$\tau^+\tau^-(\gamma)$ [$e^+e^-\mu^-\mu^-$]

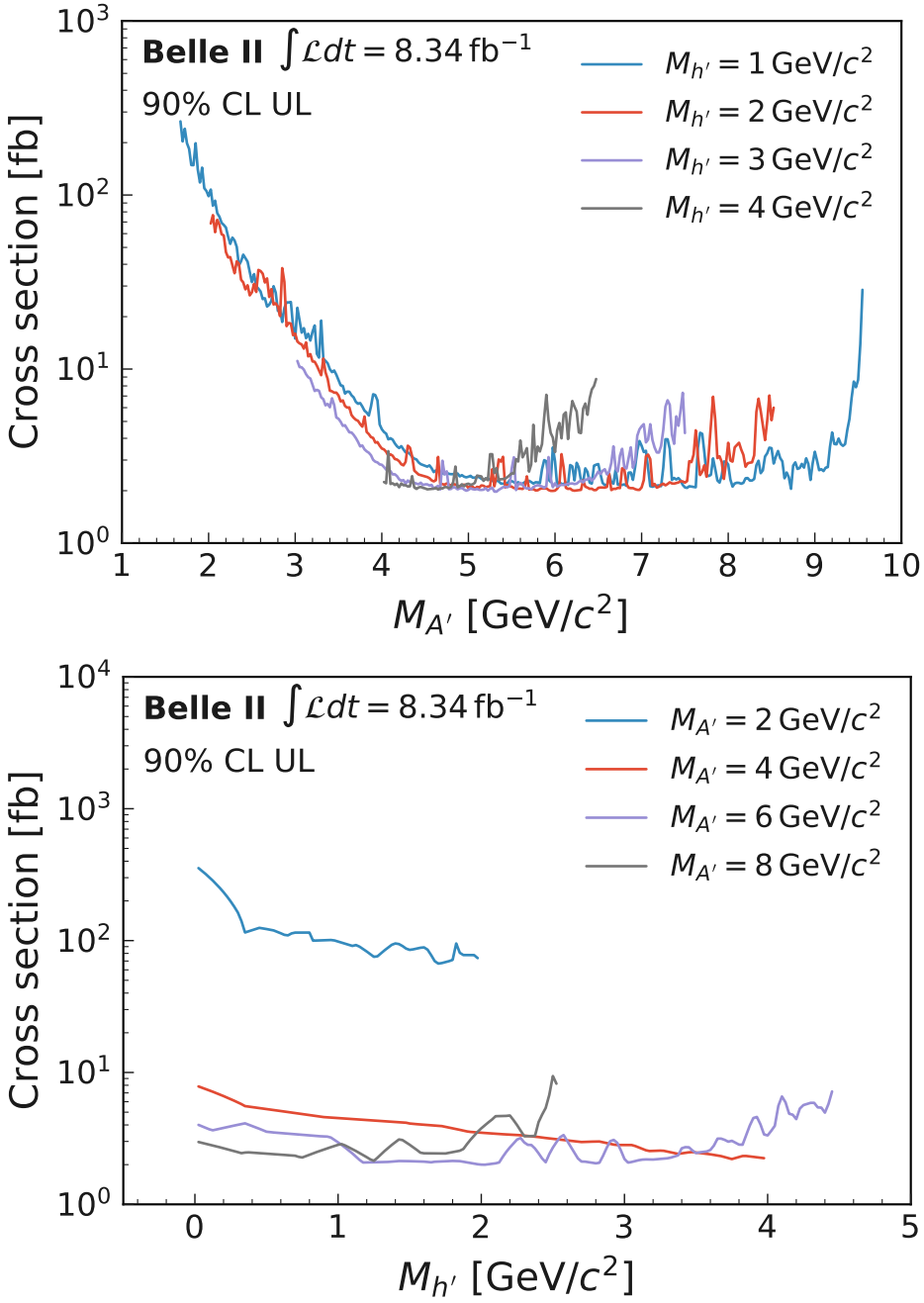

FIG. S7: Observed 90% CL upper limits on the cross section for $e^+e^- \to A'\,h'$ with $A' \to \mu^+\mu^-$ and h' invisible (*top*) as functions of $M_{A'}$ for four values of $M_{h'}$ and (*bottom*) as functions of $M_{h'}$ for four values of $M_{A'}$.

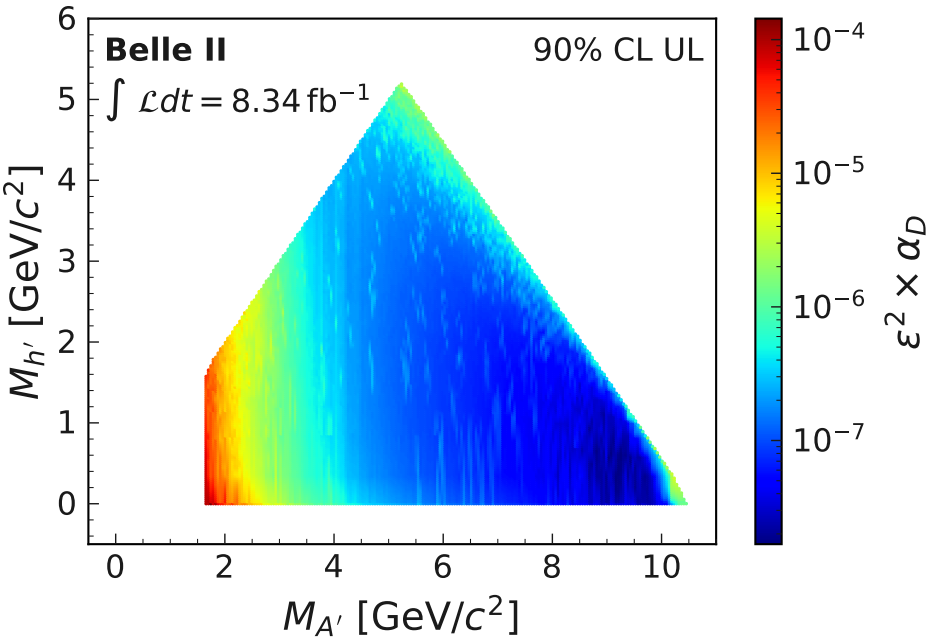

FIG. S8: Observed 90% CL upper limit on $\varepsilon^2 \times \alpha_D$ as a function of the A' and h' masses. Values are computed at search window centers and then interpolated to points of the search plane.

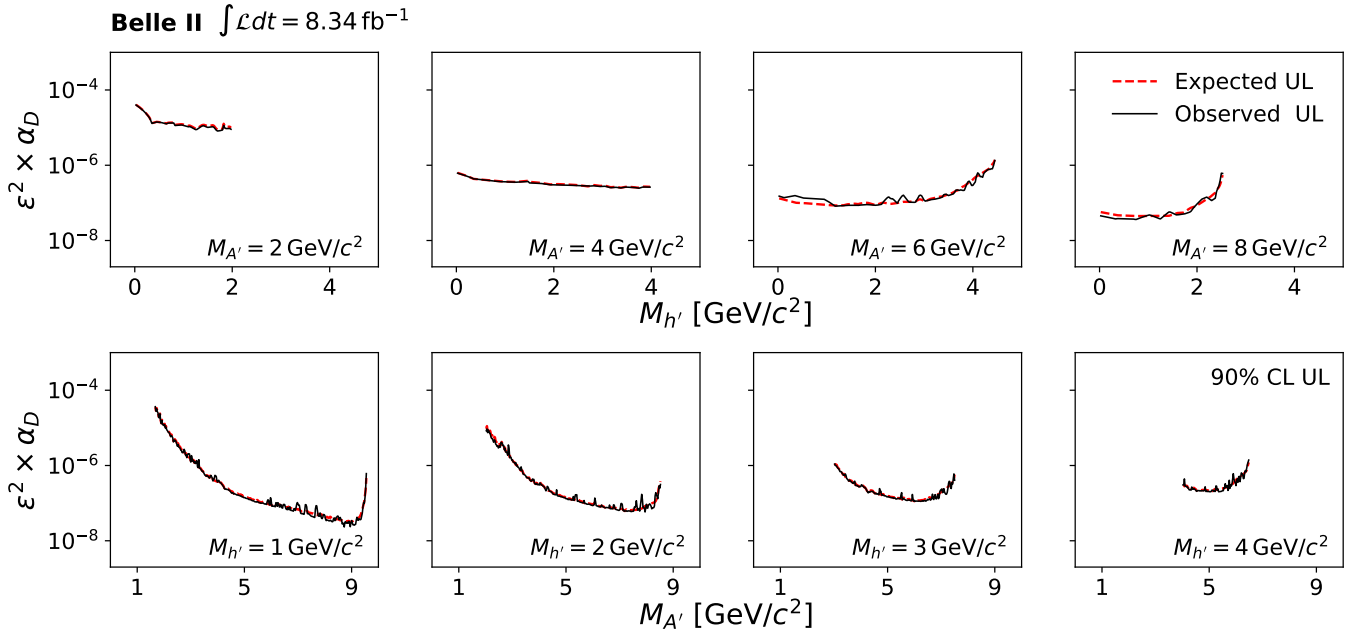

FIG. S9: Observed 90% CL upper limits on $\varepsilon^2 \times \alpha_D$ (solid black line) and their expected values (dotted red line) (*top*) as functions of $M_{h'}$ for four values of $M_{A'}$ and (*bottom*) as functions of $M_{A'}$ for four values of $M_{h'}$.